OncoTargets and Therapy

Dovepress
open access to scientific and medical research

Open Access Full Text Article

ORIGINAL RESEARCH

The SP1-Induced Long Noncoding RNA, LINC00339, Promotes Tumorigenesis in Colorectal Cancer via the miR-378a-3p/MED19 Axis

This article was published in the following Dove Press journal:
OncoTargets and Therapy

Hua Ye[1,2]
Wende Li[3]
Kefeng Wu[1,2]
Yi Liu[1,2]
Yingnian Lv[1,2]
Yuzhen Zhu[1,2]
Hui Luo[1,2]
Liao Cui[1,2]

[1]Guangdong Key Laboratory for Research and Development of Natural Drugs, Guangdong Medical University, Zhanjiang, People's Republic of China; [2]Institute of Marine Biomedical Research, Guangdong Medical University, Zhanjiang, People's Republic of China; [3]Guangdong Laboratory Animals Monitoring Institute, Zhanjiang, Guangdong 524023, People's Republic of China

Introduction: Accumulating evidence has indicated that long noncoding RNAs (lncRNAs) are pivotal regulators involved in the pathogenesis of cancer; however, the molecular mechanism of LINC00339 in colorectal cancer (CRC) remains unclear.

Methods: The quantitative real-time polymerase chain reaction for the expression of LINC00339 and miR-378a-3p and Western blots for *MED19* were performed. A dual-luciferase assay was used to investigate the interaction between LIN00339 and miR-378a-3p, as well as between miR-378a-3p and *MED19*. Cell proliferation was determined by 3-(4,5-dimethyl-2-thiazolyl)-2,5-diphenyl-2H-tetrazolium bromide (MTT) and 5-ethynyl-2′-deoxyuridine (EdU) assay. The cell cycle was analyzed by propidium iodide staining followed by flow cytometry analysis. The wound-healing and transwell invasion assays were used to evaluate cell migration and invasion.

Results: The expression of LINC00339 was significantly upregulated in CRC cells and tissues, and high LINC00339 expression indicated an advanced tumor stage. Further experiments demonstrated that *SP1* activated LINC00339 expression by binding to its promoter region. Luciferase activity and RNA pull-down assays demonstrated a direct interaction between LINC00339 and miR-378a-3p. miR-378a-3p expression was decreased in CRC samples and negatively correlated with LINC00339 expression in tumors. Gain- and loss-of-function assays indicated that LINC00339 contributed to cell proliferation, cell cycle progression, migration, and invasion, while miR-378a-3p reversed these effects. Furthermore, cotransfection of wild-type *MED19* 3′-UTR reporters and miR-378a-3p significantly reduced luciferase activity. *MED19* mRNA and protein expression was inhibited and enhanced by miR-378a-3p and LINC00339, respectively. *MED19* overexpression reversed the effect of miR-378a-3p on cellular processes. Moreover, LINC00339 promoted tumor growth in vivo and induced epithelial–mesenchymal transition (EMT) and activated the Wnt/β-catenin signaling pathway in cells.

Conclusion: Our findings demonstrate the regulatory role of the SP1/LINC00339/miR-378a-3p/MED19 axis in CRC tumorigenesis and provide novel insight into the molecular mechanism underlying CRC.

Keywords: *LINC00339*, ceRNA, miR-378a-3p, *MED19*, colorectal cancer

Correspondence: Hua Ye
Guangdong Key Laboratory for Research and Development of Natural Drugs, Guangdong Medical University, 2 Wenming East Road, Zhanjiang 524023 Guangdong Province, People's Republic of China
Email yehua339@hotmail.com

Introduction

Colorectal cancer (CRC) is a worldwide health problem, representing the fourth most common malignancy and the second most frequent cause of cancer-induced death.[1] The carcinogenesis of CRC comprises multistep genetic and epigenetic alterations, which result in dysregulation of critical signaling pathways in tumor cells.[2] Accumulating studies have provided several promising and effective biomarkers for

the diagnosis, prognosis, and treatment of CRC.[3] Therefore, exploring new targets is necessary for understanding the molecular mechanism of CRC and providing novel insights for therapeutic strategies.

Long noncoding RNAs (lncRNAs) are a class of RNA molecules with lengths greater than 200 nucleotides and limited or no protein-coding potential.[4] The emerging roles of lncRNAs have been reported as pivotal regulators of cancer biological processes, including proliferation, apoptosis, differentiation, and invasion.[5] Several lncRNAs and miRNAs have been identified and demonstrated to be related to the development of CRC. For example, NEAT1 promoted cell proliferation, migration, and invasion in CRC by regulating the stability of *DDX5* protein and activating Wnt signaling.[6] Silencing of SLCO4A1-AS1 inhibited cell proliferation, invasion, epithelial–mesenchymal transition (EMT), as well as the activity of the Wnt/β-catenin signaling pathway by impairing the stability of *β-catenin*.[7] CRNDE epigenetically suppressed the expression of *DUSP5* and *CDKN1A* by binding to *EZH2*, thus promoting cell proliferation and reducing apoptosis.[8] Our previous study revealed that epigenetically silenced miR-4500 inhibited cell proliferation and migration by targeting *HMGA2* in CRC.[9]

The most commonly reported molecular mechanism underlying lncRNA-related carcinogenesis is through acting as competing endogenous RNAs (ceRNAs) to absorb microRNAs (miRNAs) and thereby positively regulating the expression of miRNA targets.[10,11] LINC00339 promotes cell proliferation and invasion and inhibits apoptosis via *FOXM1* by targeting miR-145 in non-small cell lung cancer (NSCLC).[12] LINC00339 served as a sponge for miR-377-3p and regulated its target gene *HOXC6*, thus increasing cell growth and decreasing apoptosis in triple-negative breast cancer (TNBC).[13] LINC00339 overexpression contributed to cell proliferation and migration by sponging miR-497-5p, thereby activating *IGF1R* in pancreatic cancer;[14] however, the function and mechanism of LINC00339 in CRC have not yet been studied.

MED19, also known as lung cancer metastasis-related protein 1 (*LCMR1*), has been implicated in the malignant progression of many human cancers. *MED19* mRNA expression was upregulated in CRC, and *MED19* interference led to cell growth inhibition.[15] *MED19* was identified as a miR-214 target and is involved in miR-214-induced suppression of cell proliferation and metastasis.[16] Whether *MED19* can act as a target of other miRNAs in CRC remains unknown.

In the present study, we found that LINC00339 was significantly overexpressed in CRC cells and clinical samples. Ectopic expression of LINC00339 promoted cell proliferation, cell cycle progression, migration, and invasion in vitro and tumorigenesis in vivo, while knockdown of LINC00339 showed the opposite effects. Mechanistically, *SP1*-induced LINC00339 acted as a molecular sponge of miR-378a-3p to regulate *MED19*, ultimately activating the Wnt/β-catenin pathway.

Materials and Methods

Patients and Specimens

A total of 46 CRC patients were enrolled in this study, and all patients signed informed consent forms approved by the Ethics Committee of Guangdong Medical University. Both the tumor tissues and adjacent normal tissues were assessed by two independent pathologists. The following criteria were used to screen the samples included in this study: patients had no history of solid tumors, patients had not received chemo-and radiotherapy, the samples contained tumors (percentage of tumor cells >70%) and matched non-tumor tissues (at least 5 cm away from the edge of the cancerous region), and the follow-up data were available. All clinicopathological variables are summarized in Table 1.

Cell Culture and Treatment

Human CRC cell lines (SW480, HCT-116, HT-29, and LoVo) were obtained from American Type Culture Collection (ATCC, Manassas, VA, USA) and cultured in DMEM (Invitrogen, Carlsbad, CA, USA) supplemented with 10% fetal bovine serum (FBS, Invitrogen). Normal colon epithelial cell lines (NCM460) were obtained from the Chinese Academy of Medical Sciences (Beijing, China) and cultured in McCoy's 5A medium (Invitrogen). The cells were maintained at 37 °C in an atmosphere with 5% CO_2.

Small Interfering RNA (siRNA) Synthesis and Vector Construction

For silencing of *SP1*, siRNAs (siSP1-1, 5′-GCCA ATAGCTACTCAACTACT-3′; siSP1-2, 5′-GGGTATGTT CCTAAGGTCATT-3′) were synthesized, and nonspecific siRNA was used as a control (siNC). For LINC00339 knockdown, siRNA (si-00339, sequence: 5′-GAGCCA GAAGTTGTCCTACTA-3′) was synthesized, and a scrambled siRNA (si-ctrl) was used as a negative control for si-00339. The miR-378a-3p mimic, inhibitor, and corresponding negative control (NC) were obtained from GenePharma (Shanghai, China). For LINC00339 overexpression, the full-length cDNA of LINC00339 was

Table 1 The Correlations Between LINC00339 and Clinicopathological Features

Variables	Cases	LINC00339		P
	n=46	L, n=21	H, n=25	
Gender				0.703
Female	14	7	7	
Male	32	14	18	
Age				0.471
<55 years	18	7	11	
≥55years	28	14	14	
Drinking				0.581
No	22	11	11	
Yes	24	10	14	
TNM stage				**0.021**
I, II	20	13	7	
III	26	8	18	
Duke's				**0.019**
A	13	9	4	
B	7	4	3	
C	26	8	18	
Differentiation				0.325
High. Mod	27	14	13	
Low, un	19	7	12	

Note: P<0.05 are present in bold.
Abbreviations: No, no more than 6 times per year; Yes, more than 6 times per year; mod, moderate; un, undifferentiation; L, low expression; H, high expression.

amplified and subcloned into the KpnI and BamHI sites of the pcDNA3.1 vector (Invitrogen). The pcDNA3.1 empty vector (pc-NC) was used as a negative control for the LINC00339 overexpression vector. The shRNA for LINC00339 depletion (5′-GACAGCTCCTAGAGTATCTTAATTGAT-3′) was synthesized and inserted into the pGPH1/Neo vector (GenePharma). To generate cells stably overexpressing or silencing LINC00339, HCT-116 cells were transfected with pc-LINC00339 or sh-LINC00339, and the transfected cells were selected with 2 g/mL puromycin. For *MED19* overexpression, the full-length cDNA of *MED19* was PCR amplified and constructed into the XbaI and XhoI sites of the pcDNA3.1 vector, and an empty vector was used as a control (pc-NC). Transfection was performed using Lipofectamine 3000 (Invitrogen).

Subcellular Fractionation Assay

RNA was extracted from nuclear or cytoplasmic fractions using Nuclear and Cytoplasmic Extraction Reagents (Thermo, Waltham, MA, USA) and evaluated using RT-qPCR analysis. U6 and *GAPDH* acted as nuclear and cytoplasmic controls, respectively.

RNA Extraction and Quantitative Real-Time PCR (qRT-PCR)

Tissues and cells were lysed by TRIzol reagent (Invitrogen) according to standard protocols and subsequently reverse transcribed into cDNA using a PrimeScript Strand cDNA Synthesis Kit (TaKaRa, Japan). qRT-PCR was performed using SYBR® Premix Ex Taq™ II (Takara) in the StepOne Plus system (Applied Biosystems, Foster City, CA, USA). LINC00339 and *MED19* were normalized to *GAPDH*, and miR-378a-3p was standardized to U6. The primers used were as follows: LINC00339: 5′-AGAACTTCTCCGGAGC GAAA-3′ (forward) and 5′-TCCTCGGCCCATCATTTCAT -3′ (reverse); *MED19*: 5′-GGCTGTGGCCCTTTTTACCT-3′ (forward) and 5′-TATCATGGGAACCAGGCAGAT-3′ (reverse); and miR-378a-3p: 5′-ACUGGACUUGGAGUC AGAAGG-3′. The $2^{-\Delta\Delta Ct}$ method was used to calculate the relative expression levels of target genes.

Luciferase Reporter Assay

The *SP1* binding motif in the promoter region of LINC00339 was identified by JASPAR (http://jaspar.genereg.net/). The full-length and the different fragment sequences were synthesized and then cloned into the pGL3-basic vector (Promega, Madison, WI, USA). All vectors were verified by sequencing, and luciferase activities were assessed using the Dual Luciferase Assay Kit (Promega).

LINC00339 and *MED19* wild type (wt) with potential miR-378a-3p binding sites or mutants of each site (mut) were amplified and cloned into the psi-CHECK-2 luciferase reporter (Promega). HCT-116 cells were seeded in a 24-well plate and grown to 80% confluence. The cells were then cotransfected with luciferase reporters and miR-378a-3p or the negative control. After 48 h of transfection, luciferase activity was tested using a Dual-Luciferase Reporter Assay System (Promega).

MTT and EdU Assays

For the MTT assay, 2×10^3 cells were seeded in a 96-well plate and cultured in complete medium. Ten microliters of MTT solution (5 mg/mL) was added to each well at the indicated time points. After incubation for 4 h, 100 μL of dimethyl sulfoxide (DMSO) was added to each well to

stop the reaction. Thirty minutes later, the absorbance was measured using a microplate reader (Thermo) at 490 nm.

For the EdU assay, 4×10^3 cells were seeded in a 96-well plate, and the Cell-Light EdU Apollo 567 Kit (Ribobio, Shanghai, China) was used to evaluate cell proliferation. After removing the medium, the cells were treated with 100 μL of a 50 μM EdU solution at 37 °C for 2 h. Then, the cells were fixed with 4% paraformaldehyde for 30 min and incubated with 50 μL glycocoll for 5 min. After incubation with 100 μL of 0.5% Triton X-100 penetrant, the cells were washed with PBS and incubated with 100 μL of Apollo staining reaction at room temperature and then decolorized with methanol. The cells were visualized under a fluorescence microscope.

Cell Cycle Analysis

Flow cytometry was used to determine the cell cycle distribution. After transfection for 24 h, the cells were cultured in serum-free medium for 24 h and further fixed using 70% ethanol at 4 °C overnight. Then, the cells were incubated with propidium iodide (PI, 50 μg/mL) for 20 minutes in the dark at 37 °C. FACScan (Becton-Dickinson, Franklin Lakes, NJ, USA) was used to analyze the cells, and ModFit software (Becton-Dickinson) was used to quantify the number of cells in the different phases.

Scratch Wound Assay

The transfected cells (2×10^5 per sample) were seeded into a 6-well plate and cultured at 37 °C for 12 h. When the cells reached 90% confluence, the cells were scratched with a pipette tip in the middle of each well and further cultured for 24 h after washing. The cells were photographed under a light microscope after 36 h.

Matrigel Invasion Assay

Transwell chambers (Millipore, Boston, MA, USA) precoated with Matrigel were used to assess cell invasion. The transfected cells were suspended in serum-free medium, and 3×10^4 cells (500 μL) were added to the upper chamber. Medium containing 10% FBS was added to the lower chamber. Forty-eight hours later, the remaining cells in the upper chamber were removed by a cotton swab, and the invaded cells were washed with PBS, fixed with 4% paraformaldehyde, and stained with 0.1% crystal violet (Sigma). Three randomly selected visual fields under the microscope were used to count the number of invaded cells.

RNA Pull-Down Assay

MiR-378a-3p-wt and miR-378a-3p-mut (GeneCreate, Wuhan, China) labeled with biotin, called bio-miR-378a-3p-wt and bio-miR-378a-3p-mut, respectively, were used to transfect cells. Bio-NC was used as a negative control. The cells were incubated in lysis buffer (Ambion, Austin, Texas, USA) for 10 min. M-280 streptavidin beads (S3762, Sigma) were precoated with RNase-free bovine serum albumin (BSA) and yeast tRNA (Sigma), followed by incubation with lysate at 4 °C overnight. The cells were washed with precooled buffer, three times with low salt buffer, and once with high salt buffer. After purification of bound RNA, LINC00339 enrichment was verified by RT-qPCR.

Western Blotting

First, tissue samples and cell lysates were treated with RIPA Reagent (Beyotime, Shanghai, China), and the protein concentration was measured using a BCA kit (Thermo). Then, equal amounts of proteins were separated by SDS-PAGE and transferred onto PVDF membranes (Thermo). The membranes were blocked in 5% nonfat milk for 2 h and then incubated at 4 °C overnight with anti-E-cadherin (ab76055, Abcam, Cambridge, MA, USA), anti-N-cadherin (ab18203), anti-vimentin (ab8978, 1:500), anti-β-catenin (ab32572), anti-c-Myc (ab32072), anti-cyclin D1 (ab16663), anti-MED19 (ab179735), and anti-GAPDH (ab9484). The membranes were then washed with TBST buffer and incubated with secondary antibodies at room temperature for 2 h. The blots were visualized using ECL reagent (Amersham Biosciences, Buckinghamshire, UK).

Mouse Tumor Model

A total of 12 BALB/c nude *mice* (5 weeks old, male) were raised in specific pathogen-free conditions, and all animal procedures were approved by Guangdong Medical University and all procedures were applied in accordance with The Guide for Care and Use of Laboratory Animals, Guangdong Medical University. The nude mice were randomly grouped into the following three groups (n=4 for each group): sh-00339 (LINC00339 depletion), 00339 (LINC00339 overexpression), and blank control group. HCT-116 cells (5×10^6) were injected subcutaneously into the flanks of nude *mice*, and tumor width and length were measured once a week. The tumor xenograft volume was calculated using the formula: (length×width^2)/2. Five weeks after the injection, the mice were sacrificed, and the tumor xenografts were resected and weighed.

Immunohistochemistry (IHC) Assay

An IHC assay was used to determine the protein expression of *MED19* in 46 CRC samples and 6 randomly selected nontumor tissues. The extent of staining was classified as follows: <15% positive cells, 0; 15–30%, 1; 30–60%, 2; and >60% positive cells, 3. The intensity of staining was scored according to the following criterion: no staining, 1; weak, 2; moderate, 3; and strong, 4. The IHC staining score of *MED19* was defined as the extent multiplied by intensity (ranging from 0 to 12). A final score of no more than 4 was defined as low *MED19* expression, while a score greater than 4 was defined as high *MED19* expression.

Statistical Analysis

The data are presented as the mean ± standard deviation and were analyzed with SPSS 16.0 (IBM, Chicago, IL, USA). Statistical significance of the differences between two or more than two groups was assessed by Student's *t*-test or ANOVA. The correlations between two genes were estimated by Pearson's correlation analysis. A P value <0.05 was considered statistically significant, and every experiment was conducted at least three times.

Results

The Expression of LINC00339 in CRC Samples and Cells

First, the expression of LINC00339 was determined in CRC cells. LINC00339 was significantly overexpressed in CRC cells (HT-29, HCT-116, LoVo, SW480) compared to control NCM460 cells ($p<0.05$, Figure 1A). Further analysis showed that LINC00339 expression levels were dramatically higher in CRC tissues than in adjacent non-cancerous tissues (0.986±0.458 vs. 0.516±0.336; $p<0.001$, Figure 1B). These data suggested that LINC00339 may have important roles in CRC development.

SP1 Activates LINC00339 Transcription in CRC Cells

Accumulating evidence suggests that transcription factors such as *SP1* could activate the transcription of downstream lncRNAs.[17] After applying the JASPAR online database, we observed five putative *SP1* binding sites (E1: −1872 bp to −1882 bp; E2: −1808 bp to −1818 bp; E3: −1498 bp to −1508 bp; E4: −1306 bp −1316 bp; E5: −725 bp to −735 bp) at the promoter region of LINC00339 (relative score>0.9; Figure 2A). Then, the expression of *SP1* was silenced by siRNA interference technology in CRC (Figure 2B). After *SP1* knockdown, the expression of LINC00339 was reduced (Figure 2C). *SP1* overexpression increased the expression of LINC00339 (Figure 2D). The results of ChIP assays indicated strong *SP1*-binding activity on the LINC00339 promoter region around the E3/E4 and E5 sites (Figure 2E). In addition, to further verify the effect of *SP1* on LINC00339, pGL3-basic reporters containing the full promoter region of LINC00339, the E5 deleted promoter region, and the E3/E4/E5 deleted promoter region were constructed. We found that the effect of *SP1* on LINC00339 transcription activation was lost upon the deletion of the E3/E4 and E5 sites (Figure 2F). These data indicated that *SP1* could activate LINC00339 expression by binding to its promoter region (Figure 2).

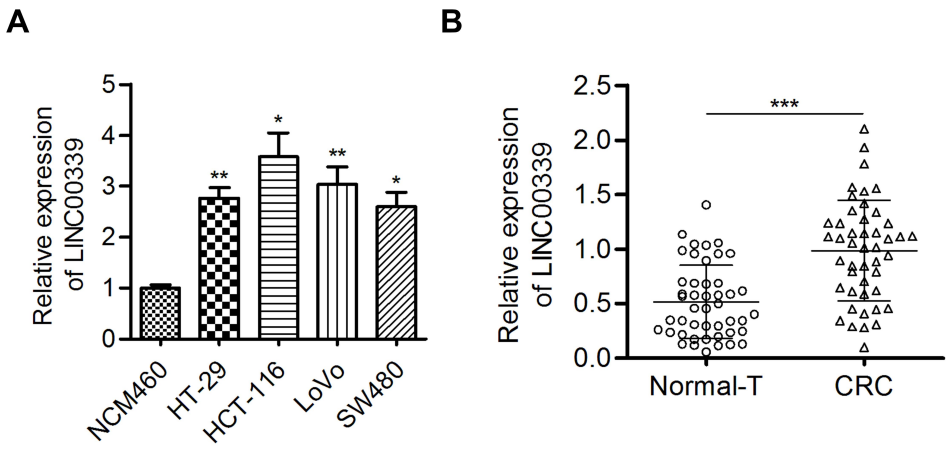

Figure 1 LINC00339 expression was increased in CRC tissues and cells.
Notes: (**A**) qRT-PCR was conducted to measure the expression of LINC00339 in CRC cells and NCM460 cells. (**B**) The expression of LINC00339 was increased in CRC tissues compared with normal control tissues. The data are presented as the mean ± standard deviation; *P<0.05. **P<0.01. ***P<0.001.
Abbreviations: CRC, colorectal cancer; Normal-T, adjacent nontumor tissues.

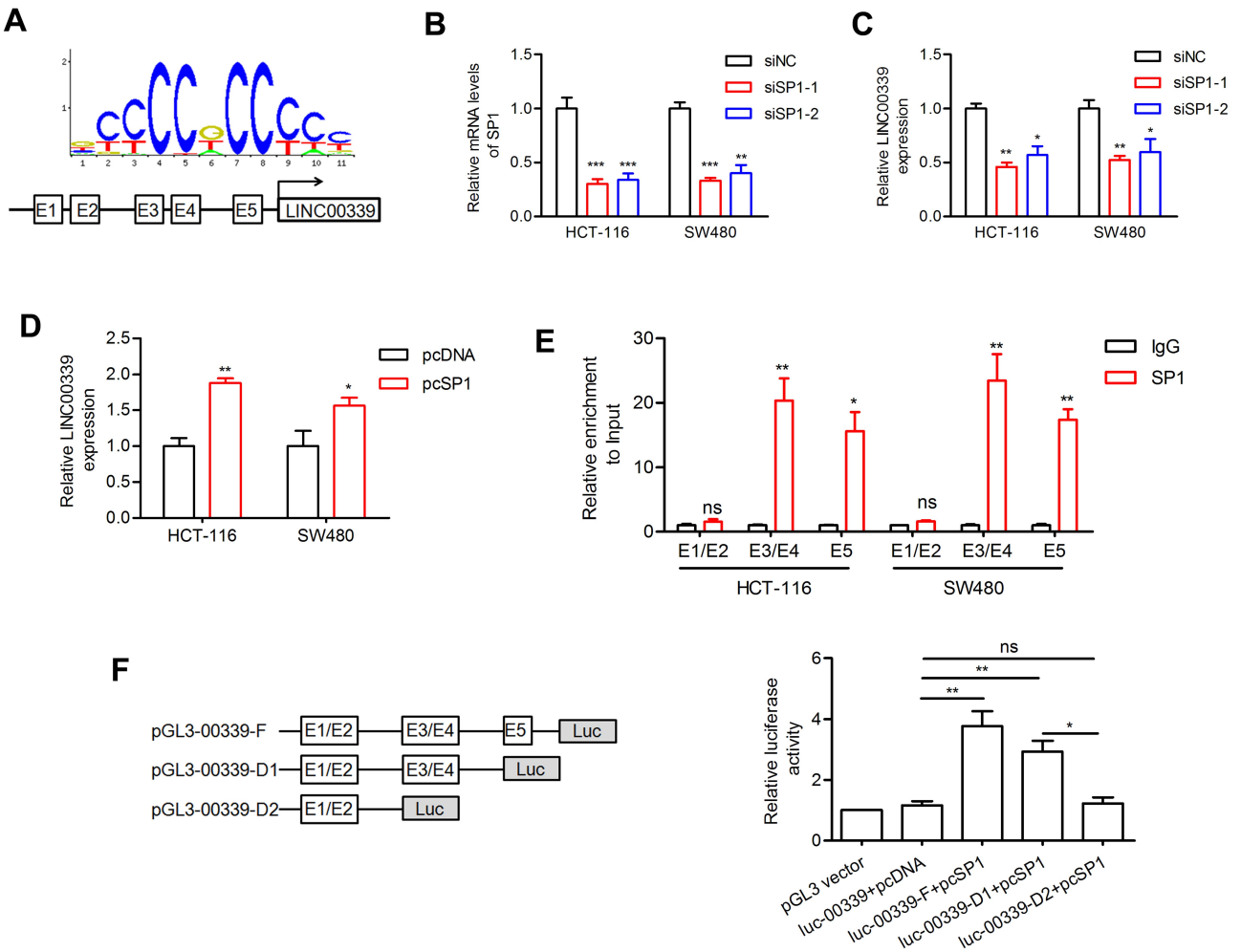

Figure 2 *SP1* activates LINC00339 expression.

Notes: (**A**) The possible binding site of SP1 on the LINC00339 promoter was predicted using JASPAR. (**B**) SP1 was silenced after transfection with siSP1-1/2 in CRC cells. (**C**) LINC00339 expression was decreased after SP1 knockdown. (**D**) SP1 overexpression activated LINC00339 expression. (**E**) ChIP assays showed that SP1 could precipitate the LINC00339 promoter fragment, including the E3/E4 and E5 regions. (**F**) A luciferase reporter assay was performed by cotransfecting the full promoter (pGL3-LINC00339-F) or the partially deleted promoter (pGL3-LINC00339-D1/2) with SP1 or blank vector in 293T cells; luciferase activities were expressed relative to the pGL3 vector. *P<0.05, **P<0.01, ***P<0.001.

Abbreviations: siSP1-1/2, siRNA specifically targeting SP1; siNC, siRNA negative control; pcSP1, SP1 overexpressing vector; pcDNA, vector control; ns, no significance.

MiR-378a-3p is a Target of LINC00339

To determine the underlying mechanism by which LINC00339 exerts its function, the subcellular location of LINC00339 was determined in HCT-116 cells. LINC00339 was located in both the cytoplasm (65%) and nucleus (35%, Figure 3A), suggesting that LINC00339 may act as a miRNA sponge. Among the candidate targets of LINC00339 predicted by lncBase v2.0, miR-330-5p, miR-149-5p, miR-422a, miR-378a-3p, miR-338-3p, and miR-143-3p were well annotated and conserved miRNAs. We preliminarily measured the effect of LINC00339 on the expression of these miRNAs. As shown in Figure 3B and C, knockdown of LINC00339 induced miR-422a, miR-143-3p, and in particular, miR-378a-3p upregulation. Thus, miR-378a-3p was selected for further analysis. MiR-378a-3p has a putative binding site on LINC00339 (Figure 3D). The luciferase activity assay indicated that miR-378a-3p overexpression impaired the wt-LINC00339 reporter but not the mut-LINC00339 reporter (Figure 3E). Likewise, cotransfection of wt-LINC00339 and the miR-378a-3p inhibitor activated luciferase activity; however, cotransfection of mut-LINC00339 and the miR-378a-3p inhibitor failed to alter luciferase activity (Figure 3E). LINC00339 was pulled down by biotinylated miR-378a-3p-wt, whereas mutation of the binding sites for miR-378a-3p in LINC00339 disrupted the interaction (Figure 3F).

In addition, miR-378a-3p reduced LINC00339 expression, whereas the miR-378a-3p inhibitor elevated LINC00339

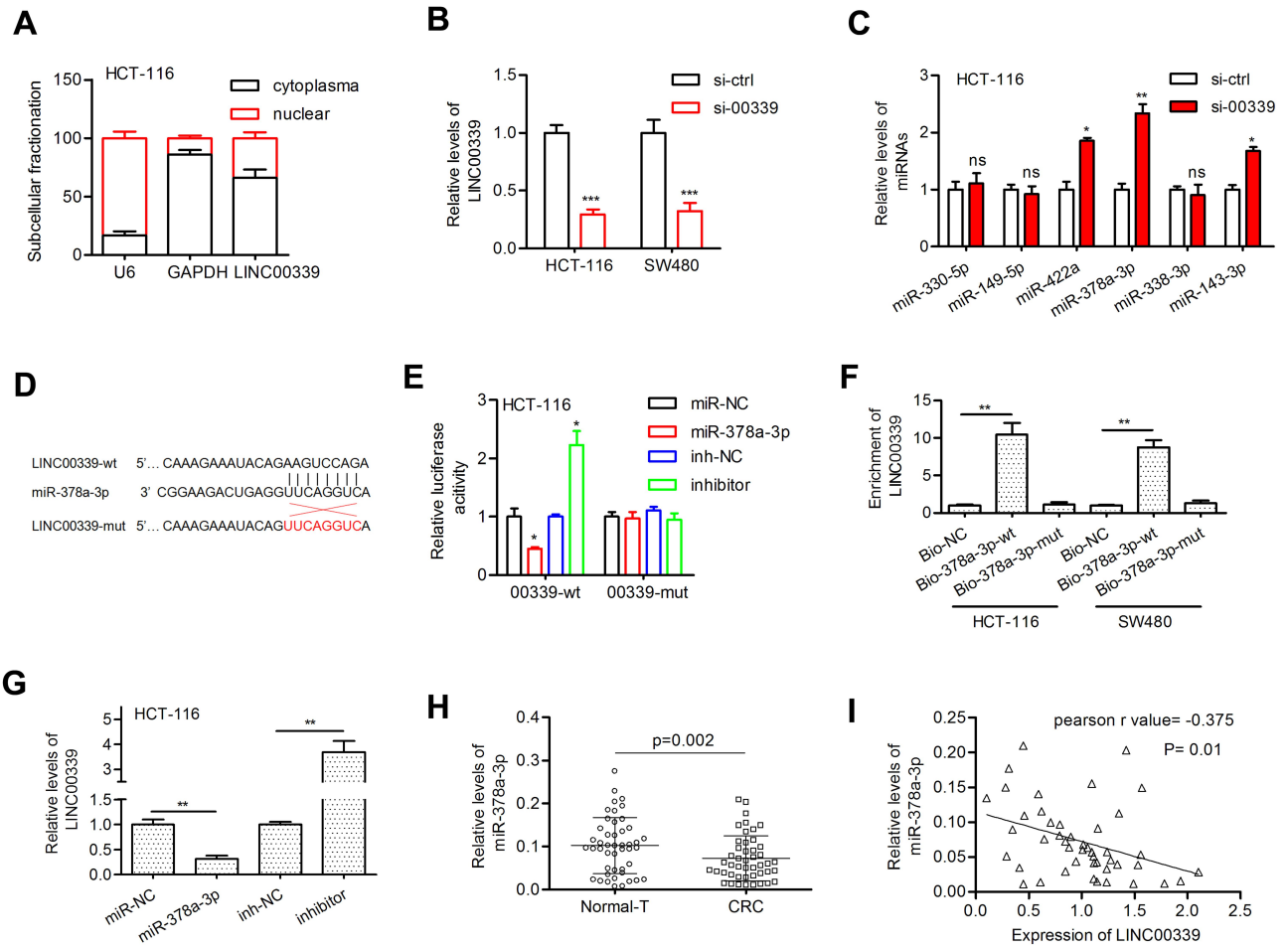

Figure 3 LINC00339 acted as a molecular sponge for miR-378a-3p.

Notes: (**A**) A subcellular fractionation assay was conducted in HCT-116 cells. (**B**) LINC00339 expression was depleted in CRC cells after transfection with si-00339. (**C**) The expression of predicted miRNAs in HCT-116 cells after transfection with si-00339. (**D**) The putative binding sites of miR-378a-3p on LINC00339 were predicted by lncBase. (**E**) MiR-378a-3p decreased the luciferase activity of wild-type LINC00339 fragments but not the mutants. (**F**) RNA pull-down assay validated the direct interaction between LINC00339 and miR-378a-3p. (**G**) The expression of LINC00339. (**H**) MiR-378a-3p levels were lower in CRC tissues than in nontumor tissues. (**I**) Statistical correlations between LINC00339 expression and miR-378a-3p were analyzed using the Pearson correlation coefficient test. *P<0.05, **P<0.01, ***P<0.001.

Abbreviations: si-ctrl, non-specific negative control of LINC00339 silencing; si-00339, specific siRNA for knocking down LINC00339; wt, wild type; mut, mutant type; NC, negative control; Normal-T, adjacent nontumor tissues.

expression in HCT-116 cells (Figure 3G). We also confirmed that the expression of miR-378a-3p was markedly downregulated in CRC tissues (0.073±0.052 vs. 0.102±0.065, p=0.002; Figure 3H), and Pearson correlation analysis revealed that miR-378a-3p expression was negatively correlated with LINC00339 expression in tumors (Pearson r=−0.375, p=0.01; Figure 3I).

MiR-378a-3p is Involved in LINC00339-Regulated Tumorigenesis

To investigate the biological role of LINC00339 and miR-378a-3p, HCT-116 cells were cotransfected with si-00339 (or si-ctrl) and inhibitor (or inh-NC), and SW480 cells were cotransfected with pc-00339 (pc-NC) and miR-378a-3p (or miR-NC) (Figure 4A). The transfection efficiency was determined by qRT-PCR assays (Figure 4B). MTT assay showed that knockdown of LINC00339 inhibited cell proliferation, while LINC00339 overexpression displayed the opposite effect. The miR-378a-3p inhibitor and miR-378a-3p mimic reversed the effect of si-00339 and pc-00339 on cell proliferation, respectively (Figure 4C). The results of the EdU assay confirmed the promotive effect of LINC00339 on cell proliferation and the inhibitory function of miR-378a-3p (Figure 4D). LINC00339 silencing induced cell cycle arrest at the G0/G1 phase, which was rescued upon inhibition of miR-378a-3p. miR-378a-3p overexpression reversed the cell cycle transition from the G0/G1 to S phase induced by LINC00339 (Figure 4E). Furthermore, wound healing assays revealed that the migratory ability of CRC cells was

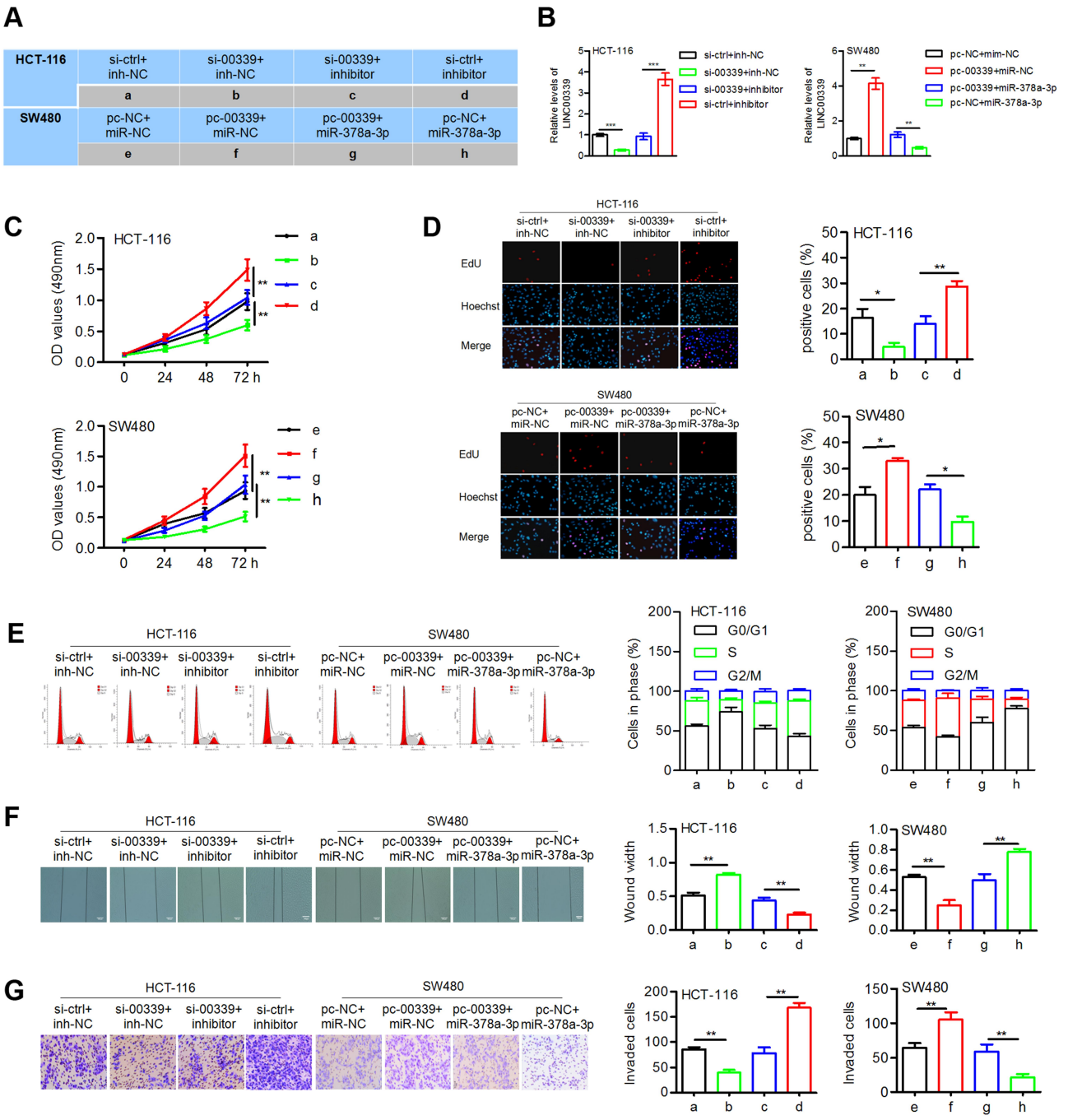

Figure 4 LINC00339 confers oncogenic properties on CRC cells by regulating miR-378a-3p.

Notes: (**A**) The different groups in the two cell lines are shown and described. (**B**) LINC00339 expression was determined in CRC cells after transfection. (**C**, **D**) MTT and EdU assays were used to test cell proliferation. (**E**) Cell cycle distribution was evaluated by flow cytometry. (**F**, **G**) Wound-healing and Transwell invasion assays were used to evaluate cell migration and invasion, respectively. *P<0.05, **P<0.01, ***P<0.001.

Abbreviations: pc-NC, vector control; pc-00339, LINC00339 overexpression plasmids; inhibitor, miR-378a-3p inhibitor; NC, negative control.

enhanced by LINC00339 and the miR-378a-3p inhibitor but suppressed by si-00339 and miR-378a-3p mimic (Figure 4F). The miR-378a-3p inhibitor attenuated the repressive function of si-00339 on cell invasiveness, and miR-378a-3p impaired the promotive effect of pc-00339 on SW480 cell invasion (Figure 4G). These data suggest that LINC00339 might exert cancer-promoting activity through by negatively regulating miR-378a-3p in CRC (Figure 4).

MED19 is a Target of miR-378a-3p

To explore the functional target of miR-378a-3p in CRC, four online prediction tools were used, and four genes,

including *GOLT1A*, *MED19*, *MAP2K6*, and *PLAGL2* (Figure 5A), attracted our attention due to their increased expression in colon adenocarcinoma (COAD) cases according to the GEPIA database (data not shown). Among those genes, *MED19* was reported to be closely related to the progression of several types of cancers, including CRC. Thus, we aimed to verify the relationship between miR-378a-3p and *MED19*. The candidate binding sites of miR-378a-3p on the 3′-UTR of *MED19* mRNA are shown in Figure 5B. Ectopic expression of miR-378a-3p significantly reduced the luciferase activity of the wt- but not that of the mut-MED19 3′-UTR (Figure 5C). Introducing LINC00339 impaired the suppressive effect of miR-378a-3p on the luciferase activity of the *MED19* mRNA 3′-UTR (Figure 5C). These results suggested that LINC00339 attenuated the miR-378a-3p-induced repression of *MED19* via competitively binding miR-378a-3p (Figure 5).

LINC00339 Positively Regulated MED19 by Sponging miR-378a-3p in CRC

Subsequently, the results of the qRT-PCR assay indicated that the mRNA levels of *MED19* were significantly reduced by miR-378a-3p but were recovered by the miR-378a-3p

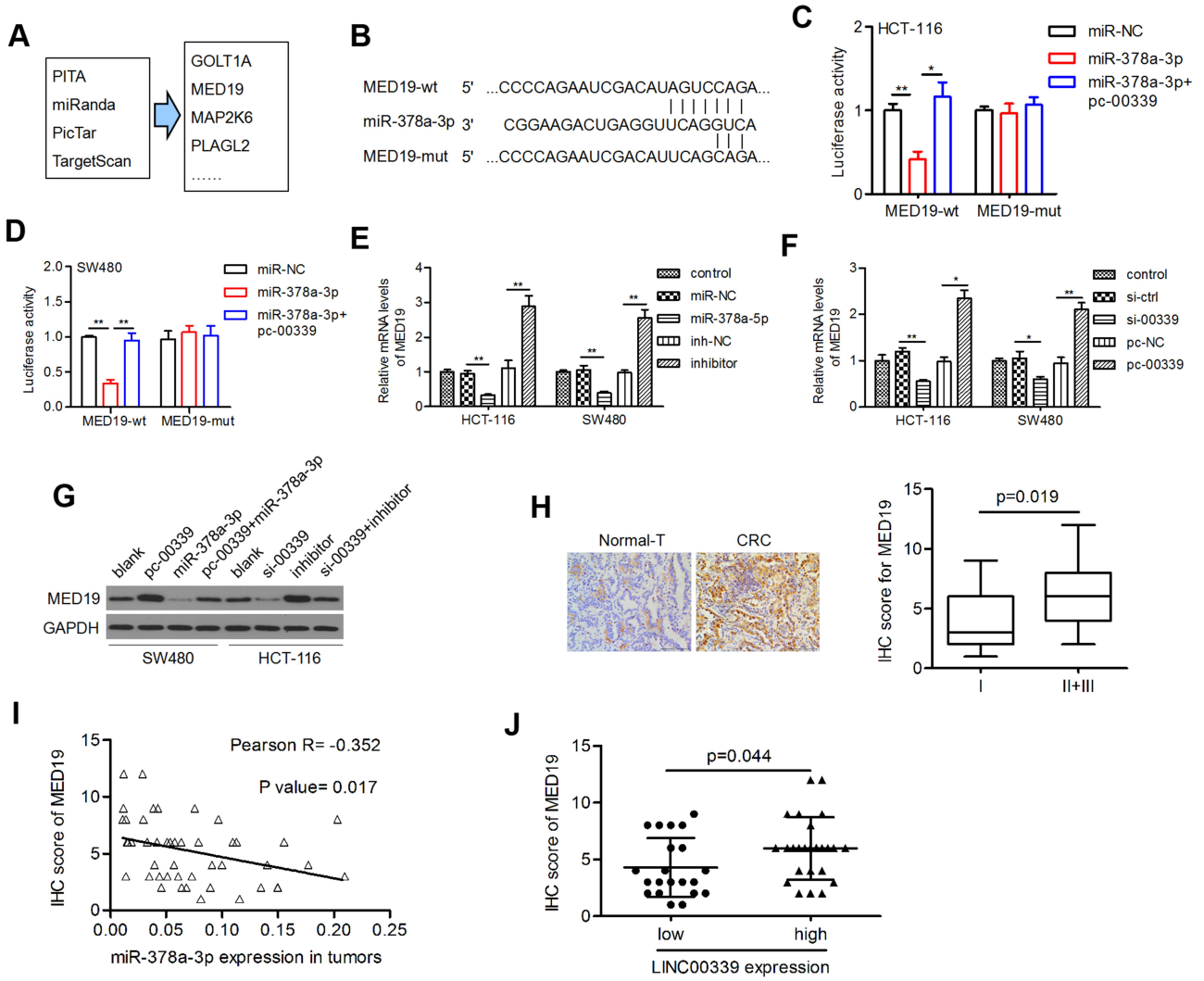

Figure 5 *MED19* was regulated by LINC00339 in a miR-378a-3p-dependent manner.

Notes: (**A**) Four online tools were used to screen the putative targets of miR-378a-3p. (**B**) The seed sequence of miR-378a-3p on MED19 mRNA 3′-UTR. (**C**, **D**) The relative luciferase activity in HCT-116 and SW480 cells; miR-378a-3p reduced the luciferase activity of wild-type MED19 3′UTR, and the introduction of LINC00339 rescued it. (**E**, **F**) The mRNA levels of MED19 were negatively and positively regulated by miR-378a-3p and LINC00339, respectively. (**G**) MiR-378a-3p is involved in LINC00339-regulated MED19 protein expression. (**H**) IHC assay was conducted in nontumor tissues (n=5) and CRC tissues (n=46), left; MED19 levels indicated a higher clinical stage, right. (**I**) The MED19 protein level in CRC was negatively correlated with miR-378a-3p expression. (**J**) A high MED19 IHC score was associated with increased LIN00339 expression in tumors. *P<0.05, **P<0.01.

Abbreviations: wt, wild type; mut, mutant type; Normal-T, adjacent nontumor tissues.

inhibitor (Figure 5D). The effects of LINC00339 depletion and overexpression on *MED19* mRNA expression were similar to those of miR-378a-3p and the inhibitor, respectively (Figure 5E). The results of the Western blot assay confirmed that miR-378a-3p abolished the LINC00339-induced *MED19* upregulation, while the miR-378a-3p inhibitor restored the LINC00339 silencing-induced suppression of *MED19* (Figure 5F).

The protein expression of *MED19* in clinical tumor tissues (n=46) and randomly selected nontumor tissues (n=6) was examined by IHC. We found that *MED19* protein was overexpressed in CRC cases compared to adjacent nontumor tissues (Figure 5G, left). When analyzing the correlation between the *MED19* staining score and the clinicopathological features of CRC cases, increased *MED19* protein expression was associated with aggressive CRC phenotypes (p=0.019; Figure 5G, right). Moreover, *MED19* protein levels were inversely correlated with miR-378a-3p expression levels in tumor tissues (Pearson r=−0.352, p=0.017, Figure 5H). *MED19* expression was higher in the LINC00339 high expression group than in the LINC00339 low expression group (p=0.044; Figure 5I), suggesting a positive correlation between LINC00339 and *MED19*.

MED19 is a Functional Target of miR-378a-3p

Two groups of cells were used for the following experiments: miR-378a-3p plus pcDNA control and miR-378a-3p plus pcMED19. The expression of *MED19* was significantly restored in pcMED19 vector-transfected cells (Figure 6A). The MTT and EdU assay results indicated that *MED19* restoration increased cell proliferation in both HCT-116 and SW480 cells (Figure 6B and C). Elevated *MED19* increased the number of cells in S phase and reduced the number of cells in G0 phase (Figure 6D). In addition, *MED19* upregulation induced cell migration and invasion in CRC cells (Figure 6E and F). These data suggest that *MED19* is a functional target of miR-378a-3p in CRC progression.

LINC00339 Promotes EMT via the Wnt/β-Catenin Pathway

We subsequently assessed the involvement of miR-378a-3p and *MED19* in accelerating EMT by activating the Wnt/β-catenin pathway. First, both LINC00339 and *MED19* overexpression led to the inhibition of E-cadherin and an increase in vimentin and N-cadherin, while miR-378a-3p exhibited the opposite effect on EMT markers (Figure 7A). The oncogenic function of LINC00339 could be attenuated by miR-378a-3p, and the suppressive role of miR-378a-3p in EMT could be reversed by *MED19* (Figure 7A), which indicated that miR-378a-3p/MED19 is involved in LINC00339-regulated EMT. LINC00339 upregulation increased the protein levels of *β-catenin*, *c-Myc*, and *cyclin D1*, while miR-378a-3p partially reversed these effects. Elevated *MED19* impaired the inhibitory role of miR-378a-3p on the protein expression of typical downstream genes of the Wnt/β-catenin pathway (Figure 7A). These results demonstrated that LINC00339 could activate the Wnt/β-catenin pathway by regulating miR-378a-3p/MED19.

LINC00339 Promotes Tumor Growth in vivo and the Progression of CRC

To further examine the oncogenic activity of LINC00339, we stably transfected HCT-116 cells with sh-LINC00339 or pc-LINC00339. The cells were then injected subcutaneously into nude mice. Elevated LINC00339 led to significantly larger tumor volumes and weights (Figure 7B–D). Depletion of LINC00339 reduced the volumes and weights of the tumors compared with the blank control group (Figure 7B–D).

Forty-six cases of CRC were separated into two groups depending on the expression levels of LINC00339 in tumor tissues: 21 cases low expression (<median value) and 25 cases of high expression (≥median value). Then, the cases were divided into several subgroups based on gender, age, and Tumor-Lymph Nodes-Metastasis (TNM) stage. We found that the expression of LINC00339 was associated with TNM staging (p=0.021) and Duke's staging (p=0.019) but not correlated with other clinicopathological features (Table 1). We also analyzed the correlations between miR-378a-3p and clinical data and found that dysregulated miR-378a-3p had no correlation with clinicopathological features. In addition, a Cox regression model was used to evaluate the impact of clinicopathological variables on patient survival. The univariate analysis results showed that three factors, including TNM stage (p=0.024, HR=3.582), Duke's stage (p=0.033, HR=8.971), and differentiation (p=0.022, HR=2.992), were associated with an increased risk of death (Table 2); however, multivariate analysis confirmed that none of the three factors were independently associated with the risk of death (Table 2).

Discussion

Recently, lncRNAs have emerged as critical regulators targeting miRNAs and affecting gene expression in

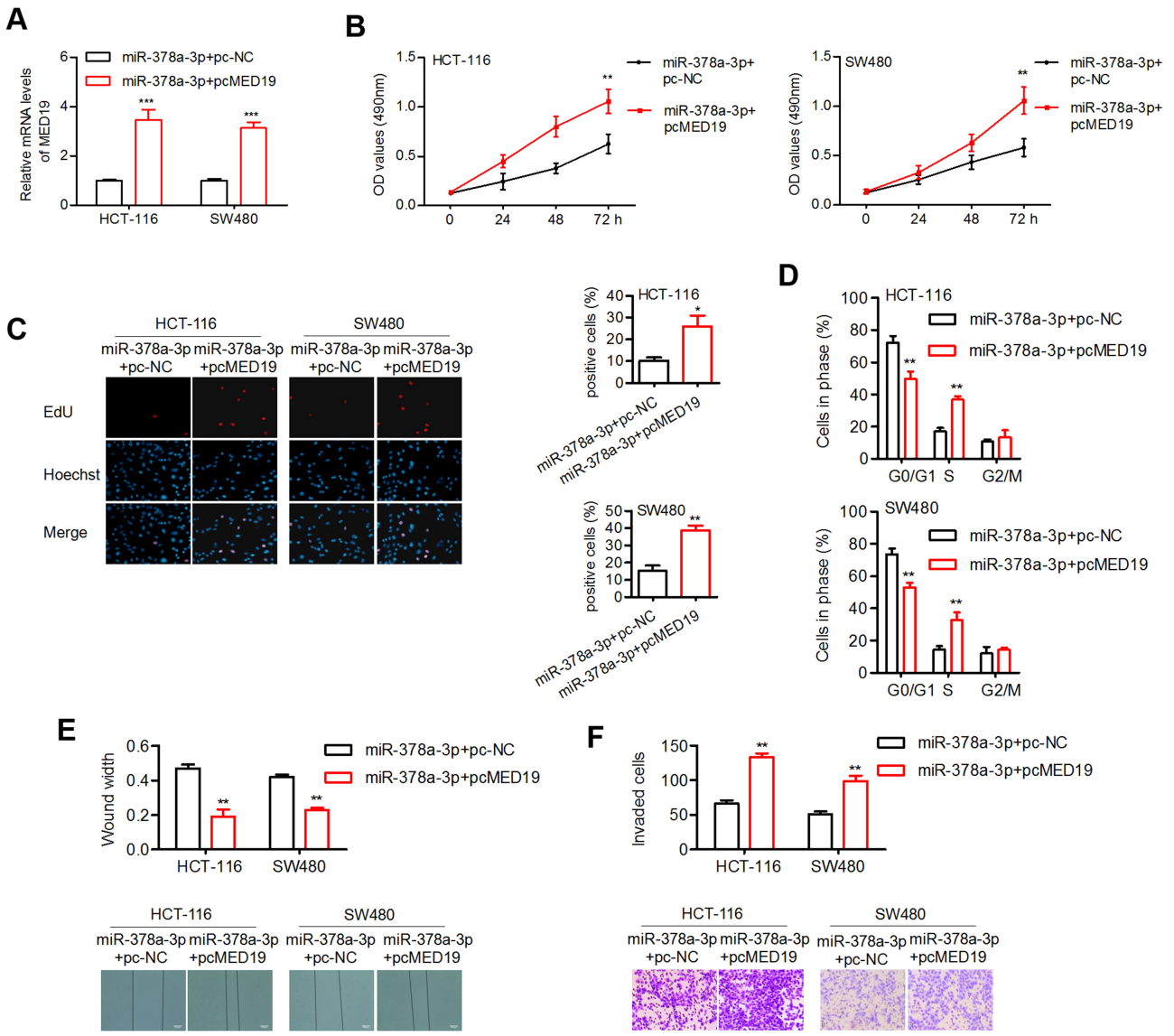

Figure 6 *MED19* reversed the effect of miR-378a-3p on cellular processes.

Notes: (**A**) The transfection efficiency was determined by qRT-PCR assay. (**B**, **C**) The MTT and EdU assay results confirmed that MED19 restoration promoted cell proliferation. (**D**) MED19 facilitated cell cycle progression from the G1 to S phase. (**E**, **F**) Cell migration and invasiveness were inhibited upon MED19 recovery. *P<0.05, **P<0.01, ***P<0.001.

Abbreviations: pc-NC, vector control; pcMED19, MED19 expressing plasmids.

multiple cancers.[18] Here, we revealed that LINC00339 was upregulated in CRC cells and primary tumors. High LINC00339 expression was associated with tumor stage but not prognosis in CRC patients. Our data expands upon the knowledge of LINC00339 in the development of CRC. LINC00339 overexpression indicated poor overall survival in patients with NSCLC and gastric cancer.[12,19] Patients with high levels of LINC003399 tend to have a significantly larger tumor size and higher tumor stage in ovarian cancer.[20] LINC00339 upregulation was associated with advanced stage, metastasis, and poor prognosis in hepatocellular carcinoma.[21] All these data indicate that LINC00339 upregulation may be a common event in most types of cancers, and LINC00339 may therefore be a promising diagnostic or prognostic marker.

The results of the subcellular fractionation assay showed that LINC00339 was more enriched in the cytoplasm than in the nucleus. Thus, we searched for candidate miRNA targets of LINC00339 in CRC cells. By using online prediction tools and a preliminary qRT-PCR test, miR-378a-3p was selected for further analysis. The results of luciferase activity and RNA pull-down assays demonstrated that miR-378a-3p is a novel target of LINC00339. The expression of LINC00339 was negatively regulated by miR-378a-3p. Moreover, the

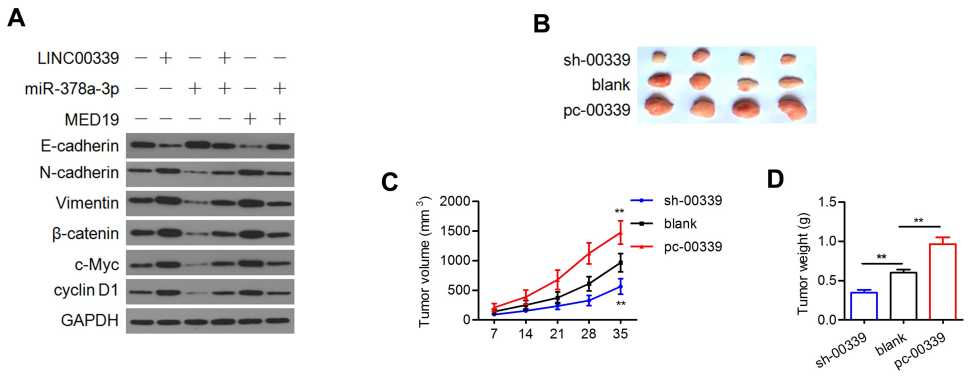

Figure 7 LINC00339 contributes to Wnt/β-catenin signaling and tumor growth.
Notes: (**A**) Western blot analysis revealed the protein expression of EMT markers and downstream genes of the Wnt/β-catenin pathway. Both EMT and Wnt/β-catenin pathway activity were increased by LINC00339 and MED19 but decreased by miR-378a-3p in HCT-116 cells. (**B**) Representative tumors obtained from different mouse groups. (**C**, **D**) Tumor volume and tumor weight were elevated by LINC00339 overexpression and reduced by LINC00339 silencing. **P<0.01
Abbreviations: sh-00339, stable depletion of LINC00339 in mice; pc-00339, stable overexpression of LINC00339 in mice; blank, no treatment group.

expression of miR-378a-3p was significantly downregulated in CRC tissues and inversely correlated with LINC00339 expression, suggesting that miR-378a-3p interacts with LINC00339 in the progression of CRC. Several miRNAs, including miR-145, miR-337-3p, miR-497-5p, miR-148a-3p, miR-152, and miR-4656, were found to be regulated by LINC00339 in different types of cancer.[12–14,20,22,23] These miRNAs provide a broader base for LINC00339 to exert its function in carcinogenesis. Gain- and loss-of-function analysis indicated that LINC00339 contributed to cell viability and motility in vitro and tumorigenesis in vivo. Our data revealed the cancer-promoting activity of LINC00339 in CRC, and similar results were also reported in other types of cancers.[12,13,22] We also found that LINC00339 activated the expression of *N-cadherin* and *vimentin* but decreased *E-cadherin* expression. LINC00339-induced EMT may be responsible for augmented cell migration and invasion. The protein expression of *β-catenin*, *c-Myc*, and *cyclin D1* was elevated by LINC00339, suggesting that the Wnt/β-catenin pathway was activated in LINC00339-related tumor biological processes. Our data indicated that LINC00339 facilitated cell proliferation, metastasis, and EMT in CRC by activating the Wnt/β-catenin pathway.

The results of the functional assay demonstrated that the oncogenic function of LINC00339 could be restrained by miR-378a-3p and that the tumor suppressive role of LINC00339 depletion could be inhibited by the miR-378a-3p inhibitor. MiR-378a-3p inhibited cell proliferation and reduced cyclin dependent kinase 4/6 (*CDK4/6*) expression in NSCLC cells.[24] The expression of miR-378a-3p was downregulated in CRC samples.[25] MiR-378a-3p was repressed by oncogenic lnc-p23154, and cell migration, invasion and glycolysis were induced by the miR-378a-3p-targeted gene *Glut1* in oral squamous cell carcinoma.[26]

Table 2 Cox Regression Model Was Used to Estimate Relationship Between Survival and Specified Variables

Variables	Subgroups	Univariate			Multivariate		
		HR	P	CI	HR	P	CI
Gender	F/M	0.683	0.448	0.255–1.828			
Age	<55/≥ 55years	2.093	0.157	0.752–5.822			
Drinking	No/Yes	1.222	0.667	0.489–3.055			
TNM stage	I+II/III	3.582	**0.024**	1.184–10.844	1.771	0.370	0.508–6.177
Duke's	A/B+C	8.971	**0.033**	1.189–67.661	4.682	0.186	0.475–46.146
Differentiation	High+mod/low+un	2.992	**0.022**	1.172–7.634	2.528	0.055	0.982–6.506
LINC00339	Low/high	1.677	0.279	0.657–4.280			
miR-378a-3p	High/low	1.196	0.708	0.468–3.054			
MED19	Low/high	2.232	0.094	0.871–5.715			

Note: P<0.05 are present in bold.
Abbreviations: F, female; M, male; No, no more than 6 times per year; Yes, more than 6 times per year; mod, moderate; un, undifferentiation; HR, hazard ratio; CI, confidence interval.

Considering the downregulated expression status of miR-378a-3p in CRC tissues, our data suggest a tumor suppressor role of miR-378a-3p in the oncogenesis of CRC.

MED19 is a predicted target of miR-378a-3p. MiR-422a, which shares the same seed sequence with miR-378a-3p, represses the expression of *MED19* by targeting its 3′-UTR in breast cancer.[27] *MED19* was negatively regulated by miR-378a-3p in cells, and its protein expression was inversely correlated with miR-378a-3p in tumor tissues. More importantly, we found that high *MED19* protein levels indicated aggressive CRC phenotypes. These data suggest that dysregulation of miR-378a-3p/MED19 may play a part in CRC progression.

In this study, ectopic *MED19* expression increased proliferation, the number of cells in S phase, migration, and invasion in both HCT-116 and SW480 cells, which is similar to previous studies.[16] miR-4778-3p reduced the proliferation and migration of radioresistant cervical cancer cells by regulating *MED19* expression.[28] In contrast, *MED19* knockdown suppressed proliferation and migration by reducing the activity of Wnt/β-catenin signaling in breast cancer.[29] *MED19* downregulation inhibited colony formation, migration, and invasion, as well as cell growth and EMT-related genes such as *p27*, *E-Cadherin*, *N-Cadherin*, *vimentin*, *snail-1* and *snail-2* in prostate cancer.[30] Interfering with *MED19* induced cell cycle arrest at the G1 phase and prohibited migration in tongue cancer cells.[31] Here, we revealed that *MED19* induced the EMT process by activating the Wnt/β-catenin pathway in CRC, providing a possible mechanism by which *MED19* affects tumorigenesis and metastasis.

In summary, we reported that LINC00339, an overexpressed lncRNA in CRC, promoted cell proliferation, cell cycle progression, migration, and invasion. We suggest that *SP1*-induced LINC00339 acts as a sponge of miR-378a-3p to positively regulate *MED19* expression, thereby activating the Wnt/β-catenin pathway and CRC carcinogenesis. LINC00339 may therefore provide possible therapeutic strategies for CRC treatment.

Acknowledgments

This study was supported by Natural Science Foundation of Guangdong Province (No. 2018A0303130252), Major scientific research projects in Colleges and universities of Guangdong (No. 2017KTSCX081), Special Supporting Project for Educational Talents in Universities (No. 4SG19057G), Medical Research Foundation of Guangdong Province (No. A2018495), Administration of Traditional Chinese Medicine of Guangdong Province (No. 20182069), and Science and Technology Fund of Zhanjiang (No. 2017A06012).

Disclosure

The authors declare that they have no conflicts of interest.

References

1. Bray F, Ferlay J, Soerjomataram I, Siegel RL, Torre LA, Jemal A. Global cancer statistics 2018: GLOBOCAN estimates of incidence and mortality worldwide for 36 cancers in 185 countries. *CA Cancer J Clin*. 2018;68(6):394–424. doi:10.3322/caac.21492
2. Hong SN. Genetic and epigenetic alterations of colorectal cancer. *Intest Res*. 2018;16(3):327–337. doi:10.5217/ir.2018.16.3.327
3. Coppedè F, Lopomo A, Spisni R, Migliore L. Genetic and epigenetic biomarkers for diagnosis, prognosis and treatment of colorectal cancer. *World J Gastroenterol*. 2014;20(4):943–956. doi:10.3748/wjg.v20.i4.943
4. Guttman M, Rinn JL. Modular regulatory principles of large non-coding RNAs. *Nature*. 2012;482(7385):339–346. doi:10.1038/nature10887
5. Hosseini ES, Meryet-Figuiere M, Sabzalipoor H, Kashani HH, Nikzad H, Asemi Z. Dysregulated expression of long noncoding RNAs in gynecologic cancers. *Mol Cancer*. 2017;16(1):107. doi:10.1186/s12943-017-0671-2
6. Zhang M, Weng W, Zhang Q, et al. The lncRNA NEAT1 activates Wnt/β-catenin signaling and promotes colorectal cancer progression via interacting with DDX5. *J Hematol Oncol*. 2018;11(1):113. doi:10.1186/s13045-018-0656-7
7. Yu J, Han Z, Sun Z, Wang Y, Zheng M, Song C. LncRNA SLCO4A1-AS1 facilitates growth and metastasis of colorectal cancer through β-catenin-dependent Wnt pathway. *J Exp Clin Cancer Res*. 2018;37(1):222. doi:10.1186/s13046-018-0896-y
8. Ding J, Li J, Wang H, et al. Long noncoding RNA CRNDE promotes colorectal cancer cell proliferation via epigenetically silencing DUSP5/CDKN1A expression. *Cell Death Dis*. 2017;8(8):e2997. doi:10.1038/cddis.2017.328
9. Yu FY, Tu Y, Deng Y, et al. MiR-4500 is epigenetically downregulated in colorectal cancer and functions as a novel tumor suppressor by regulating HMGA2. *Cancer Biol Ther*. 2016;17(11):1149–1157. doi:10.1080/15384047.2016.1235661
10. Ding D, Li C, Zhao T, Li D, Yang L, Zhang B. LncRNA H19/miR-29b-3p/PGRN axis promoted epithelial-mesenchymal transition of colorectal cancer cells by acting on Wnt signaling. *Mol Cells*. 2018;41(5):423–435.
11. Wang L, Cho KB, Li Y, Tao G, Xie Z, Guo B. Long noncoding RNA (lncRNA)-mediated competing endogenous RNA networks provide novel potential biomarkers and therapeutic targets for colorectal cancer. *Int J Mol Sci*. 2019;20(22):5758. doi:10.3390/ijms20225758
12. Yuan Y, Haiying G, Zhuo L, Ying L, Xin H. Long non-coding RNA LINC00339 facilitates the tumorigenesis of non-small cell lung cancer by sponging miR-145 through targeting FOXM1. *Biomed Pharmacother*. 2018;105:707–713. doi:10.1016/j.biopha.2018.06.022
13. Wang X, Chen T, Zhang Y, et al. Long noncoding RNA Linc00339 promotes triple-negative breast cancer progression through miR-377-3p/HOXC6 signaling pathway. *J Cell Physiol*. 2019;234(8):13303–13317. doi:10.1002/jcp.28007
14. Zhang R, Hao S, Yang L, Xie J, Chen S, Gu G. LINC00339 promotes cell proliferation and metastasis in pancreatic cancer via miR-497-5p/IGF1R axis. *J BUON*. 2019;24(2):729–738.
15. Jifu E, Xing JJ, Hao LQ, Fu CG. Suppression of lung cancer metastasis-related protein 1 (LCMR1) inhibits the growth of colorectal cancer cells. *Mol Biol Rep*. 2012;39(4):3675–3681. doi:10.1007/s11033-011-1142-2

16. He GY, Hu JL, Zhou L, et al. The FOXD3/miR-214/MED19 axis suppresses tumour growth and metastasis in human colorectal cancer. *Br J Cancer*. 2016;115(11):1367–1378. doi:10.1038/bjc.2016.362
17. Yu S, Wang D, Shao Y, et al. SP1-induced lncRNA TINCR overexpression contributes to colorectal cancer progression by sponging miR-7-5p. *Aging (Albany NY)*. 2019;11(5):1389–1403. doi:10.18632/aging.101839
18. Wang W, Zhou R, Wu Y, et al. PVT1 promotes cancer progression via MicroRNAs. *Front Oncol*. 2019;9:609. doi:10.3389/fonc.2019.00609
19. Shi C, Liu T, Chi J, et al. LINC00339 promotes gastric cancer progression by elevating DCP1A expression via inhibiting miR-377-3p. *J Cell Physiol*. 2019;234(12):23667–23674. doi:10.1002/jcp.28934
20. Pan L, Meng Q, Li H, Liang K, Li B. LINC00339 promotes cell proliferation, migration, and invasion of ovarian cancer cells via miR-148a-3p/ROCK1 axes. *Biomed Pharmacother*. 2019;120:109423. doi:10.1016/j.biopha.2019.109423
21. Xiao J, Yu H, Ma Z. LINC00339 promotes growth and invasiveness of hepatocellular carcinoma by the miR-1182/SKA1 pathway. *Onco Targets Ther*. 2019;12:4481–4488. doi:10.2147/OTT.S207397
22. Chen K, Zhang L. LINC00339 regulates ROCK1 by miR-152 to promote cell proliferation and migration in hepatocellular carcinoma. *J Cell Biochem*. 2019;120(9):14431–14443. doi:10.1002/jcb.28701
23. Wang W, Wang X, Li C, et al. Huaier suppresses breast cancer progression via linc00339/miR-4656/CSNK2B signaling pathway. *Front Oncol*. 2019;9:1195. doi:10.3389/fonc.2019.01195
24. Wang M, Sun X, Yang Y, Jiao W. Long non-coding RNA OIP5-AS1 promotes proliferation of lung cancer cells and leads to poor prognosis by targeting miR-378a-3p. *Thorac Cancer*. 2018;9(8):939–949. doi:10.1111/1759-7714.12767
25. Gungormez C, Gumushan Aktas H, Dilsiz N, Borazan E. Novel miRNAs as potential biomarkers in stage II colon cancer: microarray analysis. *Mol Biol Rep*. 2019;46(4):4175–4183. doi:10.1007/s11033-019-04868-7
26. Wang Y, Zhang X, Wang Z, et al. LncRNA-p23154 promotes the invasion-metastasis potential of oral squamous cell carcinoma by regulating Glut1-mediated glycolysis. *Cancer Lett*. 2018;434:172–183. doi:10.1016/j.canlet.2018.07.016
27. Zhang X, Gao D, Fang K, Guo Z, Li L. Med19 is targeted by miR-101-3p/miR-422a and promotes breast cancer progression by regulating the EGFR/MEK/ERK signaling pathway. *Cancer Lett*. 2019;444:105–115. doi:10.1016/j.canlet.2018.12.008
28. Zhang Y, Li P, Hu J, et al. Role and mechanism of miR-4778-3p and its targets NR2C2 and Med19 in cervical cancer radioresistance. *Biochem Biophys Res Commun*. 2019;508(1):210–216. doi:10.1016/j.bbrc.2018.11.110
29. Yuan H, Yu S, Cui Y, et al. Knockdown of mediator subunit Med19 suppresses bladder cancer cell proliferation and migration by down-regulating Wnt/β-catenin signalling pathway. *J Cell Mol Med*. 2017;21(12):3254–3263. doi:10.1111/jcmm.13229
30. Yu S, Wang Y, Yuan H, et al. Knockdown of mediator complex subunit 19 suppresses the growth and invasion of prostate cancer cells. *PLoS One*. 2017;12(1):e0171134. doi:10.1371/journal.pone.0171134
31. Zhu LJ, Yan WX, Chen ZW, et al. Disruption of mediator complex subunit 19 (Med19) inhibits cell growth and migration in tongue cancer. *World J Surg Oncol*. 2013;11:116. doi:10.1186/1477-7819-11-116